

A proposal on the galaxy intrinsic alignment self-calibration in weak lensing surveys

Pengjie Zhang¹

¹Key Laboratory for Research in Galaxies and Cosmology, Shanghai Astronomical Observatory, Nandan Road 80, Shanghai, 200030, China; pjzhang@shao.ac.cn

30 November 2021

ABSTRACT

The galaxy intrinsic alignment causes the galaxy ellipticity-ellipticity power spectrum between two photometric redshifts to decrease faster with respect to the redshift separation Δz^P , for fixed mean redshift. This offers a valuable diagnosis on the intrinsic alignment. We show that the distinctive dependences of the GG, II and GI correlations on Δz^P over the range $|\Delta z^P| \lesssim 0.2$ can be understood robustly without strong assumptions on the intrinsic alignment. This allows us to measure the intrinsic alignment within each conventional photo- z bin of typical size $\gtrsim 0.2$, through lensing tomography of photo- z bin size ~ 0.01 . Both the statistical and systematical errors in the lensing cosmology can be reduced by this self-calibration technique.

Key words: cosmology: gravitational lensing–theory: large scale structure

1 INTRODUCTION

The galaxy intrinsic alignment (IA) is one of the major systematical errors of cosmic shear measurement. The intrinsic alignment of physically close galaxy pairs is correlated due to the tidal force arising from the correlated large scale structure and thus induces the intrinsic ellipticity-intrinsic ellipticity correlation (the II correlation). Due to the same reason, it is also correlated with the ambient matter distribution, which lenses background galaxies within sufficiently small angular separation and hence couples the shape of background galaxies with the shape of foreground galaxies, even if the galaxy pairs are widely separated in redshift. This induces the gravitational shear-intrinsic ellipticity correlation (the GI correlation, Hirata & Seljak 2004). Various methods have been proposed to correct for the II correlation (King & Schneider 2002, 2003; Heymans & Heavens 2003; Takada & White 2004; Okumura et al. 2009) and the GI correlation (Hirata & Seljak 2004; Heymans et al. 2006; Joachimi & Schneider 2008; Zhang 2008; Joachimi & Schneider 2009; Joachimi & Bridle 2009; Okumura & Jing 2009; Kirk et al. 2010; Shi et al. 2010; Joachimi & Schneider 2010).

Here we point out a new possibility to self-calibrate the intrinsic alignment. It is known that the lensing signal GG and the contaminations II and GI have different dependences on the pair separation Δz^P . This has motivated the proposals to reduce the II correlation by using only cross correlation between thick photo- z bins of size $\gtrsim 0.2$ (e.g. Takada & White 2004).

What we will show in this paper is that, these dependences can be understood robustly over the range $|\Delta z^P| \lesssim$

0.2 without heavy IA modeling. *This allows us to self-calibrate the intrinsic alignment with basically no assumptions on the intrinsic alignment, through lensing tomography of fine photo- z bin size ~ 0.01 within each conventional photo- z bin of size $\gtrsim 0.2$.* With this self-calibration technique, we no longer need to throw away the auto-correlation measurement of each conventional thick photo- z bins. It will bring in two-fold improvement on cosmology. First, it directly improves the cosmological constraints by $O(10\%)$ (Takada & White 2004), since the auto-correlation measurement can now be safely included. The price to pay is orders of magnitude more correlation measurements due to many more photo- z bins. Second, it extracts valuable information on the intrinsic alignment within each thick photo- z bin, which helps calibrate the intrinsic alignment in the cross correlation measurement. This new proposal, along with existing ones (e.g. King & Schneider 2002; Bridle & King 2007; Joachimi & Schneider 2008; Zhang 2008; Bernstein 2009; Joachimi & Schneider 2009, 2010), demonstrate the rich information brought in by the photo- z measurement to reduce systematical errors and to improve cosmological constraints, which is otherwise lost in the usual lensing tomography of thick photo- z bins.

The current proposal is complementary to other model independent methods, especially the nulling technique proposed by Joachimi & Schneider (2008, 2009, 2010). Our method takes advantage of the characteristic Δz^P dependences of the lensing signal and the intrinsic alignment, for a fixed mean source redshift \bar{z}^P , to separate the two. Over the interesting range $|\Delta z^P| \lesssim 0.2$, since the lensing geometry kernel is wide, the lensing signal barely changes as a

function of Δz^P while both II and GI change significantly. On the other hand, the nulling technique uses the characteristic z^P dependence of the lensing signal, arising from the lensing geometry kernel, to suppress IA by a proper weighting function of z^P . It relies on significant variation of the lensing kernel with respect to z^P over sufficiently large redshift range. Hence the two methods are highly complementary and we expect significant improvement in calibrating the intrinsic alignment by combining the two methods.

2 THE Δz^P DEPENDENCES

We work on the power spectrum $C^{\alpha\beta}(\ell, z_1^P, z_2^P)$ between a property α at photo- z z_1^P and another property β at z_2^P . Here, the superscripts (and subscripts sometime) $\alpha, \beta = G, I, g$. ‘‘G’’ denotes the lensing convergence κ or the underlying 3D matter distribution, ‘‘I’’ the E-mode intrinsic ellipticity and ‘‘g’’, the 2D or 3D galaxy number over-density. Throughout this paper, we focus on the $\Delta z^P \equiv z_2^P - z_1^P$ dependence with fixed multipole ℓ and the mean redshift $\bar{z}^P \equiv (z_1^P + z_2^P)/2$. Thus we will use the notation

$$C^{\alpha\beta}(\Delta z^P | \ell, \bar{z}^P) \equiv C^{\alpha\beta}(\ell, z_1^P, z_2^P) \quad (1)$$

and often neglect the arguments ℓ and \bar{z}^P . There is an obvious symmetry $C^{\alpha\beta}(\Delta z^P) = C^{\beta\alpha}(-\Delta z^P)$. It tells us $\partial C^{\alpha\alpha} / \partial \Delta z^P |_0 = 0$, a result which will become useful later. Unless otherwise specified, we will fix $\bar{z}^P = 1.0$ and $\ell = 10^3$, both are typical choices in weak lensing statistics. We adopt the Limber approximation to evaluate $C^{\alpha\beta}$ in the standard flat Λ CDM cosmology,

$$C^{\alpha\beta}(\Delta z^P | \ell, \bar{z}^P) = \frac{2\pi^2}{\ell^3} \int_0^\infty \Delta_{\alpha\beta}^2 \left(k = \frac{\ell}{\chi(z)}, z \right) \times W_{\alpha\beta}(z, \Delta z^P, \bar{z}^P) \chi(z) H(z) dz. \quad (2)$$

Here, $\Delta_{\alpha\beta}^2(k, z)$ is the corresponding 3D power spectrum variance. $\chi(z)$ and $H(z)$ are the comoving angular diameter distance and the Hubble parameter respectively. The weighting function

$$W_{\alpha\beta}(z, \Delta z^P, \bar{z}^P) \equiv W_\alpha(z, z_1^P) W_\beta(z, z_2^P), \quad (3)$$

$$W_G(z, z^P) \equiv H^{-1}(z) \int_0^\infty W_L(z, z_s) p(z_s | z^P) dz_s, \quad (4)$$

$$W_I(z, z^P) = W_g(z, z^P) = p(z | z^P). \quad (5)$$

Here, $W_L(z, z_s)$ is the lensing kernel for a source at z_s and a lens at z . $p(z | z^P)$ is the photo- z PDF, modeled as the sum of two Gaussians (e.g. Ma & Bernstein 2008),

$$p(z | z^P) = \frac{1 - p_{\text{cat}}}{2\pi\sigma_1(z^P)} \exp\left[-\frac{(z - z^P)^2}{2\sigma_1^2(z^P)}\right] + \frac{p_{\text{cat}}}{2\pi\sigma_2(z^P)} \exp\left[-\frac{(z - f_{\text{bias}}z^P)^2}{2\sigma_2^2(z^P)}\right]. \quad (6)$$

p_{cat} is the fraction of outlier galaxies, whose true redshift is biased by a factor f_{bias} . We adopt $\sigma_{1,2}(z^P) = 0.05(1 + z^P)$ and $f_{\text{bias}} = 0.5$. This toy model roughly represents $p(z | z^P \sim 1)$ of a stage IV lensing survey (e.g. Bernstein & Huterer 2009). Stage IV dark energy surveys require $p_{\text{cat}} < 0.1\%$ (Hearin et al. 2010). However, we adopt a much more conservative $p_{\text{cat}} = 2\%$. Due to the possible photo- z scatters,

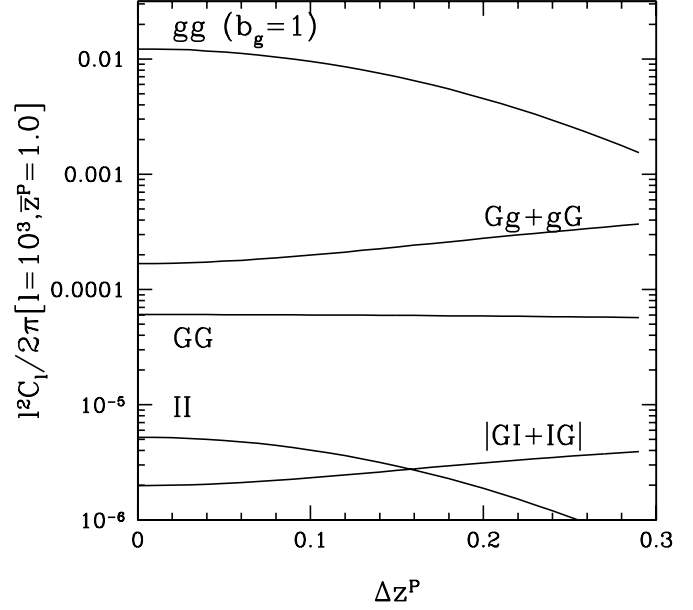


Figure 1. The power spectra $C^{\alpha\beta}(\Delta z^P | \ell = 10^3, \bar{z}^P = 1)$. We adopt the SB09 model to evaluate the II and GI correlations. Both II and GI vary with the pair separation Δz^P in ways significantly different from the lensing signal, a key for the intrinsic alignment diagnosis.

especially the catastrophic error, $C^{GI}(\ell, z_1^P, z_2^P)$ can be non-zero even if $z_1^P < z_2^P$ and $C^{IG}(\ell, z_1^P, z_2^P)$ can be non-zero even if $z_1^P > z_2^P$. So the GI contamination that we refer throughout the paper is actually the sum of the two, $C^{GI} + C^{IG}$.

To proceed, we adopt the IA model of Schneider & Bridle (2009) (hereafter SB09), based on the halo model prescription, as our fiducial model. SB09 provides a fitting formula which allows us to conveniently perform the numerical calculation. We adopt the fiducial parameters of the fitting formula listed in SB09 (and also Kirk et al. 2010) to calculate Δ_{II}^2 , Δ_{GI}^2 and hence C^{II} and C^{GI} .

$C^{\alpha\beta}$ show distinctive dependence on Δz^P (Fig. 1). Both II and GI vary by $\sim 20\%$ from $\Delta z^P = 0.0$ to $\Delta z^P = 0.1$ and by $\sim 60\%$ from $\Delta z^P = 0.0$ to $\Delta z^P = 0.2$. In sharp contrast, C^{GG} only decreases by 3% from $\Delta z^P = 0.0$ to $\Delta z^P = 0.2$. In another word, the Δz^P dependences of the II and GI correlations are more than an order of magnitude stronger than that of the signal GG. This suggests that, if the intrinsic alignment contaminates the galaxy ellipticity-ellipticity power spectrum $C^{(1)}$ by a few percent, it would cause significantly different Δz^P dependence, comparing to the case where the intrinsic alignment is ignored, in

$$C^{(1)}(\Delta z^P) = C^{GG}(\Delta z^P) + C^{II}(\Delta z^P) + C^{GI}(\Delta z^P) + C^{IG}(\Delta z^P). \quad (7)$$

The II term obviously causes $C^{(1)}$ to decrease faster than the case without the II term. Since the GI term ($= C^{GI} + C^{IG}$) has a negative sign, the increment of its amplitude with Δz^P means that it also causes $C^{(1)}$ to decrease faster. Thus

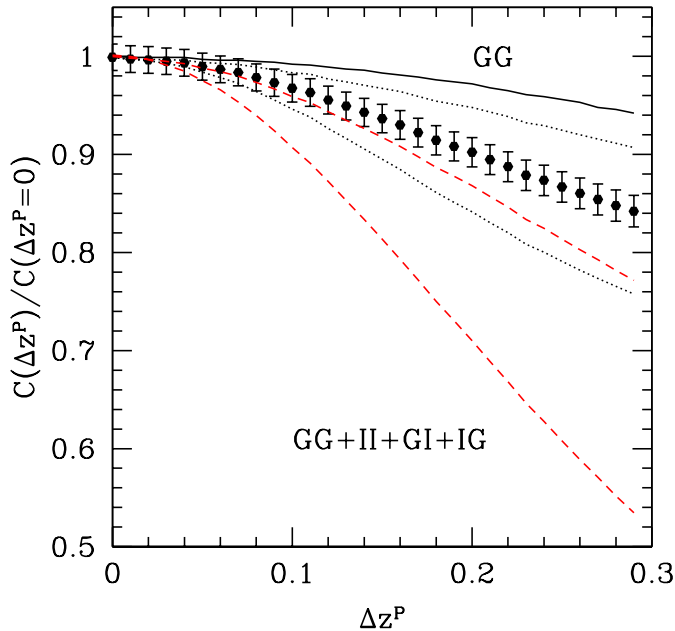


Figure 2. Diagnose the intrinsic alignment through the Δz^P dependence of the galaxy ellipticity-ellipticity power spectrum. The data points result from the fiducial SB09 model and the error estimation is for LSST. The two dot lines have 50% weaker or stronger intrinsic alignment respectively. The solid line is the ideal case of no intrinsic alignment. The two dash lines are the results of an intrinsic alignment toy model with $\gamma = 1/2$. The intrinsic alignment of the lower one is a factor of 2 stronger than the upper one. Results of other values of γ have similar behavior.

the intrinsic alignment always causes $C^{(1)}$ to decrease faster with respect to Δz^P (Fig. 2). For example, for the SB09 model, $C^{(1)}$ decreases by 10% to $\Delta z^P = 0.2$, comparing to the 3% decrease in C^{GG} .

To assess the generality of the above behavior, we also investigate a toy model. In this toy model, the intrinsic alignment has a bias (with respect to matter distribution) $b_{Im}(k, z) \propto [1 + \Delta_m^2(k, z)]^\gamma$ ($\gamma \in [0, 1/2]$) and the cross correlation coefficient $r = -1$. Here, $\Delta_m^2(k, z) \equiv \Delta_{GG}^2(k, z)$ is the 3D matter power spectrum. For this set up, $\Delta_{II}^2 = b_{Im}^2 \Delta_m^2$ and $\Delta_{IG}^2 = \Delta_{GI}^2 = b_{Im} r \Delta_m^2 = -b_{Im} \Delta_m^2$. There is no solid physics behind this toy model. But roughly speaking, $\gamma = 0$ mimics a class of IA models with linear dependence on the matter overdensity and $\gamma = 1/2$ with quadratic dependence. By choosing different γ we can cover a wide range of IA scale and redshift dependence. Over $\gamma \in [0, 1/2]$, we confirm the behavior that the intrinsic alignment causes $C^{(1)}$ to decrease faster with respect to Δz^P (Fig. 2).

This faster than usual decrease is a smoking gun of the intrinsic alignment. However, this smoking gun survives only when the photo- z performance is reasonably good. For example, if the photo- z measurement is completely wrong, with no correlation with the true redshift at all, the Δz^P dependence would vanish. Fortunately, Fig. 2 shows that, for typical photo- z performance accessible to stage IV projects, the Δz^P dependence is largely preserved, even at $\Delta z^P \lesssim 0.1$. The usual lensing tomography with coarse redshift bins of

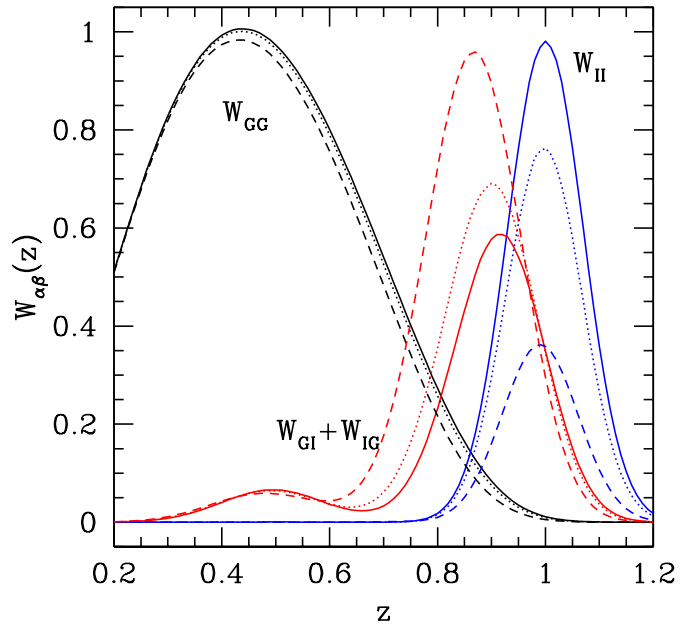


Figure 3. The weighting function $W_{\alpha\beta}(z, \Delta z^P, \bar{z}^P = 1)$. The normalizations are fixed only within each $\alpha\beta$. The lines peak at left (black lines), middle (red lines) and right (blue) are W_{GG} , $W_{GI} + W_{IG}$ and W_{II} , respectively. Solid, dot and dash lines have $\Delta z^P = 0.0, 0.1, 0.2$ respectively. The small bumps at $z \simeq 0.5$ of $W_{GI} + W_{IG}$ are caused by the combined effect of the photo- z outlier at $z \sim 0.5$ and the lensing peak at $z \sim 0.5$. They have only weak dependence on Δz^P .

size $\gtrsim 0.2$ thus misses the valuable information of the Δz^P dependence at $\Delta z^P \lesssim 0.2$. Such information can be recovered by lensing tomography with fine bin size ~ 0.01 within each coarse bin, albeit requiring two orders of magnitude more computations.

LSST and other surveys of comparable capability are able to measure the Δz^P dependence over $|\Delta z^P| \lesssim 0.2$ to desired accuracy. To a good approximation, $C^{\alpha\beta}$ at different Δz^P samples the same cosmic variances. The relative differences are then $\ll (\ell \Delta \ell f_{\text{sky}})^{-1/2} = 0.3\% (10^3/\ell)^{1/2} (100/\Delta \ell)^{1/2} f_{\text{sky}}^{1/2}$, not a limiting factor to measure the Δz^P dependence.

The *random* galaxy shape shot noise dominates over the cosmic variance at $\ell \gtrsim 10^2$, for a photo- z bin of size 0.01 at $\bar{z}^P = 1$ with 2.5×10^7 galaxies, a typical number for LSST (Zhan et al. 2009). Furthermore, since shot noises are uncorrelated at different Δz^P , it becomes more difficult to measure the Δz^P dependence. However, since the Δz^P dependence has only weak dependences on ℓ and \bar{z}^P , we can adopt a wide bin size $\Delta \ell = 500$ and average over 10 of these measurements of the same Δz^P but different $\bar{z}^P \in [0.95, 1.05]$ to beat down the shot noise to percent level, sufficient to diagnose IA and distinguish between some IA models of interest (Fig. 2).

3 UNDERSTANDING THE Δz^P DEPENDENCES

Eq. 2 shows that, $C^{\alpha\beta}(\ell, \Delta z^P, \bar{z}^P)$ of the same ℓ and \bar{z}^P samples the same 3D clustering $\Delta_{\alpha\beta}^2$, but with different weighting function $W_{\alpha\beta}$, which is the only function in the integrand depending on Δz^P . Hence the Δz^P dependence in $C^{\alpha\beta}$, especially the ratio $C(\Delta z^P)/C(\Delta z^P = 0)$, should be mainly determined by the Δz^P dependence in $W_{\alpha\beta}$, but not $\Delta_{\alpha\beta}^2$. This simple fact turns out to be highly valuable. (1) It allows us to understand the Δz^P dependence in C^{GG} to 0.1% accuracy (§3.1). (2) It allows us to understand the Δz^P dependences in C^{II} (§3.2) and C^{GI} (§3.3) without strong assumptions on the intrinsic alignment, since $W_{\alpha\beta}$ does not depend on the property of the intrinsic alignment. These are keys towards a model-independent intrinsic alignment self-calibration (§4).

3.1 The Δz^P dependence in C^{GG}

$W_{GG}(z, \Delta z^P, \bar{z}^P)$ peaks at half the distance to the source. Although the peak amplitude is sensitive to \bar{z}^P , it only weakly depends on Δz^P and only decreases by a few percent from $\Delta z^P = 0$ to $\Delta z^P = 0.2$. This explains the weak dependence of C^{GG} on Δz^P , which can be well described by the Taylor expansion around $\Delta z^P = 0$ up to second order. since $\partial C^{GG}/\partial \Delta z^P|_0 = 0$,

$$\frac{C^{GG}(\Delta z^P)}{C^{GG}(\Delta z^P = 0)} \simeq 1 - f_{GG}(\ell, \bar{z}^P)(\Delta z^P)^2, \quad (8)$$

$$f_{GG}(\ell, \bar{z}^P) \equiv \frac{\partial^2 C^{GG}(\Delta z^P)/\partial (\Delta z^P)^2|_0}{C^{GG}(\Delta z^P = 0)}.$$

We find that, $f_{GG} \in (0.5, 1.0)$ for $\ell \in [20, 4000]$ and $\bar{z}^P = 1$. At $\ell = 10^3$, $f_{GG} = 0.7$. Eq. 8 is accuracy to 0.1% up to $\Delta z^P = 0.3$.

3.2 The Δz^P dependence in the II correlation

$W_{II}(z, \Delta z^P, \bar{z}^P)$ peaks sharply at a true redshift z_{peak} (in our case, $z_{\text{peak}} \simeq 1$). The peak position is insensitive to Δz^P , although it is sensitive to \bar{z}^P , as long as the photo- z measurement is sufficiently accurate. The peak amplitude decreases with $|\Delta z^P|$ quickly, causing the sharp decrease in C^{II} at $|\Delta z^P| \gg 0.1$. This behavior is well known in the literature and has been applied to reduce the II correlation by using only the cross power spectra between thick photo- z bins, corresponding to the limit of $|\Delta z^P| \gg 0.1$. Instead, here we explore the II behavior at $|\Delta z^P| \lesssim 0.2$, namely within each thick photo- z bin of conventional lensing tomography.

Since W_{II} has a dominant and narrow peak whose position z_{peak} is insensitive to Δz^P ,

$$C^{II}(\Delta z^P | \ell, \bar{z}^P) \simeq \frac{2\pi^2 \chi(z_{\text{peak}}) H(z_{\text{peak}})}{\ell^3} \Delta_{II}^2(k, z) \times \int_0^\infty W_{II}(z, \Delta z^P, \bar{z}^P) dz. \quad (9)$$

Here, $\Delta_{II}^2(k, z)$ is evaluated at $k = \ell/\chi(z)$ and $z = z_{\text{peak}}$. The Δz^P dependence is completely described by the last integral. In the limit that $p_{\text{cat}} \rightarrow 0$ and the dependence of σ_1 on z^P is negligible, the predicted dependence becomes exact.

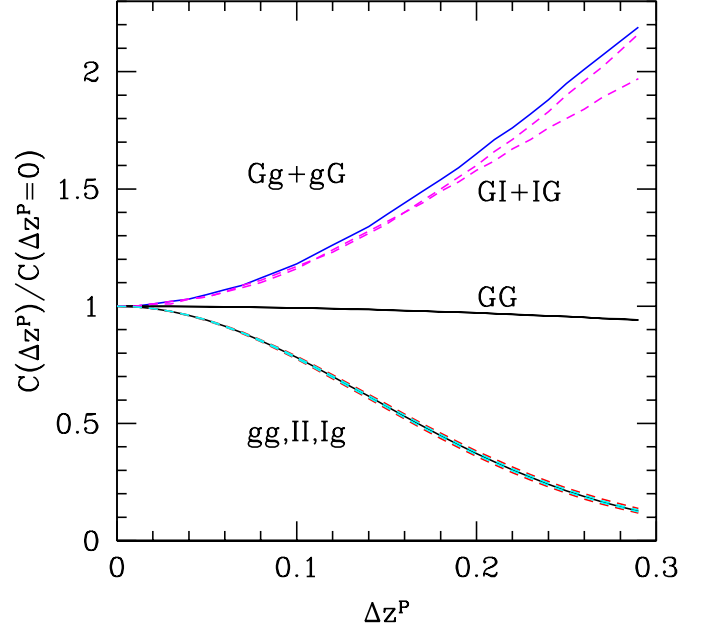


Figure 4. The accuracy of the scaling relation Eq. 8, 10, 11 & 12. The two lines labeled with “GG” are the left and right hand sides of Eq. 8. Eq. 8 is accurate to 0.1% and thus the two lines overlap. The intrinsic alignment models demonstrated are the SB09 model and the toy model with $\gamma = 1/2$. The toy models with $\gamma < 1/2$ result in better accuracy of the scaling relation. Eq. 10 & 11 are accurate to $\sim 1\%$ so the lines labeled with “gg,II,Ig” overlap. The upper solid line (blue) is $C^{Gg} + C^{gG}$. The two dash (magenta) lines labeled with “GI+IG” are the SB09 model (lower one) and the toy model with $\gamma = 1/2$ (upper one). Eq. 12 is accurate to better than $\sim 5\%$ at $\Delta z^P \leq 0.2$.

Furthermore, since $W_{II} = W_{gg}$, we suggest the following relation

$$C^{II}(\Delta z^P | \ell, \bar{z}^P) \simeq A_{II}(\ell, \bar{z}^P) C^{gg}(\Delta z^P | \ell, \bar{z}^P), \quad (10)$$

meaning the same Δz^P dependence in C^{II} and C^{gg} . This relation is not only more accurate in general, but also more useful. The same lensing survey measures $C^{gg}(\Delta z^P)$ and thus tells the Δz^P dependence in C^{II} , without external knowledge on $p(z|z^P)$ nor the intrinsic alignment. For basically the same reason, we also have

$$C^{Ig}(\Delta z^P | \ell, \bar{z}^P) \simeq A_{Ig}(\ell, \bar{z}^P) C^{gg}(\Delta z^P | \ell, \bar{z}^P). \quad (11)$$

Eq. 10 & 11 are accurate to 1%, for the SB09 model and the toy model (Fig. 4). To avoid modeling uncertainty in A_{II} and A_{Ig} (and A_{GI} in next subsection), we treat them as free parameters in the proposed self-calibration.

3.3 The Δz^P dependence in the GI correlation

The corresponding weighting function for the GI correlation ($C^{GI} + C^{IG}$) is $W_{GI} + W_{IG}$. It peaks at redshift lower than \bar{z}^P . When Δz^P increases, the true redshift separation between source and lens increases and $W_{GI} + W_{IG}$ increases. Thus the amplitude of the GI correlation ($|C^{GI} + C^{IG}|$) increases with Δz^P . Due to the peak feature in $W_{GI} + W_{IG}$,

we postulate

$$C^{GI}(\Delta z^P | \ell, \bar{z}^P) + C^{IG}(\Delta z^P | \ell, \bar{z}^P) \simeq A_{GI}(\ell, \bar{z}^P) \times [C^{Gg}(\Delta z^P | \ell, \bar{z}^P) + C^{gG}(\Delta z^P | \ell, \bar{z}^P)]. \quad (12)$$

Since the peak is not as sharp as the one in W_{II} and the peak position does move with respect to Δz^P , and since the contribution from those outlier galaxies at $z \sim 0.5$ becomes non-negligible (Fig. 3), the accuracy of Eq. 12 is not as good as Eq. 10, however, it still reaches $\sim 10\%$ up to $\Delta z^P = 0.2$ (Fig. 4). We thus take a conservative approach by restricting the self-calibration technique to $\Delta z^P \lesssim 0.2$. For this reason, performing fine binning of size 0.01 within coarse bin of size $\gtrsim 0.2$ suffices. However, if we can improve the accuracy of Eq. 12 beyond $\Delta z^P = 0.2$, binning the whole redshift range into fine bins of $\Delta z^P \sim 0.01$ would be beneficial.

The above results demonstrate that the scaling relations 10, 11 & 12 are indeed the manifestations of their corresponding weighting functions, which do not rely on the IA properties. The scale and redshift dependences of the IA clustering property are significantly different between the toy model and the SB09 model, further suggesting the generality of the above Δz^P dependences. Improvements over 10, 11 & 12, if necessary, can in principle be achieved by the theory of Gaussian quadratures (Press et al. 1997).

4 SELF-CALIBRATING THE INTRINSIC ALIGNMENT

The discovered scaling relations (Eq. 8, 10, 11 & 12) can be conveniently plugged into existing framework of lensing tomography analysis to self-calibrate the intrinsic alignment. Basically, lensing surveys allow for the measurement of the Δz^P dependences in $C^{(1)}$ (Eq. 7), $C^{(2)}$ (the ellipticity-galaxy density power spectrum) and $C^{(3)}$ (the galaxy density-galaxy density correlation power spectrum) (Hu & Jain 2004; Bernstein 2009; Zhang 2008),¹

$$\begin{aligned} C^{(2)}(\Delta z^P) &= C^{Gg}(\Delta z^P) + C^{gG}(\Delta z^P) + 2C^{Ig}(\Delta z^P), \\ C^{(3)}(\Delta z^P) &= C^{gg}(\Delta z^P). \end{aligned} \quad (13)$$

One can show that, with the aid of Eq. 8, 10, 11 & 12, measurements at 4 or more Δz^P allow for simultaneous reconstruction of GG, II, GI and free parameter f_{GG} , A_{GI} , A_{II} and A_{Ig} .

The total contamination (II+GI) in $C^{(1)}$ (Eq. 7) can be measured with higher accuracy than II or GI, since both causes $C^{(1)}$ to decrease faster and are thus partly degenerate. Basically, a 3% IA contamination in $C^{(1)}$ would double the Δz^P dependence, observable by LSST (Fig. 2) or other surveys with comparable capability.

Although we focus on $\ell = 10^3$ and $\bar{z}^P = 1$, the self-calibration proposal is applicable to other redshifts and angular scales. For example, it may work better at larger scales $\ell \sim 10^2$, where shot noise is less an issue. It may also work

with the presence of other errors, such as the PSF, which should have different Δz^P dependences.

The intrinsic alignment may also induce a non-negligible B-mode shape distortion (e.g. Heymans et al. 2006), whose power spectrum should have virtually the same Δz^P dependence as C^{gg} and differ significantly from those of other B-mode sources. This offers an independent way to diagnose IA from the B-mode shape distortion measurement, although extra modeling is required to use this B-mode measurement to correct for the E-mode IA.

The self-calibration proposal rely on no external measurement nor strong IA assumptions. In this *letter* we present a concept study on its feasibility. Quantitative analysis on its performance, along with comprehensive investigation on various complexities in realistic surveys, shall be carried out to robustly evaluate this proposal.

Acknowledgments: The author thank Gary Bernstein, Scott Dodelson and Bhuvnesh Jain for useful suggestions. This work is supported by the one-hundred talents program of the Chinese Academy of Sciences (CAS), the national science foundation of China (grant No. 10821302 & 10973027), the CAS/SAFEA International Partnership Program for Creative Research Teams and the 973 program (grant No. 2007CB815401).

REFERENCES

- Bernstein, G. M. 2009, ApJ, 695, 652
 Bernstein, G., & Huterer, D. 2009, arXiv:0902.2782
 Bridle, S., & King, L. 2007, New Journal of Physics, 9, 444
 Hearin, A. P., Zentner, A. R., Ma, Z., & Huterer, D. 2010, arXiv:1002.3383
 Heymans, C., & Heavens, A. 2003, MNRAS, 339, 711
 Heymans, C., Brown, M., Heavens, A., Meisenheimer, K., Taylor, A., & Wolf, C. 2004, MNRAS, 347, 895
 Heymans, C., White, M., Heavens, A., Vale, C., & van Waerbeke, L. 2006, MNRAS, 371, 750
 Hirata, C. M., & Seljak, U. 2004, PRD, 70, 063526
 Hu, W., & Jain, B. 2004, PRD, 70, 043009
 Joachimi, B., & Schneider, P. 2008, AAP, 488, 829
 Joachimi, B., & Schneider, P. 2009, 2009, AAP, 507, 105.
 Joachimi, B., & Schneider, P. 2010, arXiv:1003.4211
 Joachimi, B., & Bridle, S. L. 2009, arXiv:0911.2454
 King, L., & Schneider, P. 2002, AAP, 396, 411
 King, L. J., & Schneider, P. 2003, AAP, 398, 23
 Kirk, D., Bridle, S., & Schneider, M. 2010, arXiv:1001.3787
 Ma, Z., & Bernstein, G. 2008, ApJ, 682, 39
 Press, W. et al. 1997, *Numerical Recipes in Fortran 77*, Cambridge university press
 Okumura, T., Jing, Y. P., & Li, C. 2009, ApJ, 694, 214
 Okumura, T., & Jing, Y. P. 2009, ApJ, 694, L83
 Schneider, M. D., & Bridle, S. 2009, arXiv:0903.3870
 Shi, X., Joachimi, B., & Schneider, P. 2010, arXiv:1002.0693
 Takada, M., & White, M. 2004, ApJ, 601, L1
 Zhan, H., Knox, L., & Tyson, J. A. 2009, ApJ, 690, 923
 Zhang, P. 2008, arXiv:0811.0613

¹ The magnification bias can add non-negligible corrections proportional to C^{Gg} , C^{Ig} & C^{GG} to Eq. 13. Since none of them is new unknown, it does not invalidate the self-calibration, although measurement error in the galaxy luminosity function does bring new uncertainties.